

# Explaining PAMELA and WMAP data through Coannihilations in Extended SUGRA with Collider Implications

Daniel Feldman,<sup>1,2</sup> Zuowei Liu,<sup>3</sup> Pran Nath<sup>1</sup>, and Brent D. Nelson<sup>1</sup>

<sup>1</sup>*Department of Physics, Northeastern University, Boston, MA 02115, USA*

<sup>2</sup>*Address after August 1st: Michigan Center for Theoretical Physics,  
University of Michigan, Ann Arbor, MI 48109, USA*

<sup>3</sup>*C. N. Yang Institute for Theoretical Physics,  
Stony Brook University, Stony Brook, NY 11794, USA*

The PAMELA positron excess is analyzed within the framework of nonuniversal SUGRA models with an extended  $U(1)^n$  gauge symmetry in the hidden sector leading to neutralino dark matter with either a mixed Higgsino-wino LSP or an essentially pure wino dominated LSP. The Higgsino-wino LSP can produce the observed PAMELA positron excess and satisfy relic density constraints in the extended class of models due to a near degeneracy of the mass spectrum of the extended neutralino sector with the LSP mass. The simultaneous satisfaction of the WMAP relic density data and the PAMELA data is accomplished through a co-annihilation mechanism ( $B_{Co}$  - mechanism), and leads to predictions of a neutralino and a chargino in the mass range (180-200) GeV as well as low lying sparticles accessible at colliders. We show that the models are consistent with the anti-proton constraints from PAMELA as well as the photon flux data from EGRET and FERMI-LAT. Predictions for the scalar neutralino proton cross section relevant for the direct detection of dark matter are also discussed and signatures at the LHC for these PAMELA inspired models are analyzed. It is shown that the mixed Higgsino-wino LSP model will be discoverable with as little as  $1 \text{ fb}^{-1}$  of data and is thus a prime candidate for discovery in the low luminosity runs at the LHC.

PACS numbers: 12.60.Jv, 14.80.Ly, 95.35.+d

## I. INTRODUCTION

The recent results from the PAMELA experiment [1] which indicate a large excess in positron production in the galactic halo, along with a lack of any significant excess in the anti-proton flux in the same experiment, have resulted in a large effort to understand the data. Further, the results from the FERMI-LAT experiment [2] relating to the electron and photon fluxes emanating from the galaxy have also recently been reported and several interpretations have been put forth. These include particle physics models [3, 4, 5, 6, 7, 8, 9, 10, 11, 12] as well as models where the source of the PAMELA excess is of astrophysical origin [13]. Here, we give an analysis of the positron excess in a supergravity (SUGRA) framework with the neutralino as the lightest R-parity odd supersymmetric particle (LSP), where we go beyond the parameter space of the minimal supergravity grand unification model [14]. As pointed out in Ref. [15], annihilations of neutralinos into  $W^+W^-$  and their subsequent decay can provide a positron excess. One outstanding issue in supersymmetric interpretations of the positron excess has been that models with large neutralino annihilation rates into  $W^+W^-$  states tend to imply a thermally-produced cold dark matter relic density which is as much as 100 times smaller than the amount indicated by the recent WMAP data [16]. This problem has been dis-

cussed in the context of a non-thermal mechanism which is capable of generating the right amount of the relic density [4, 5]. Such non-thermal mechanisms could take place via moduli decay which can arise in various softly broken supersymmetric theories [17].

In this paper we consider an alternative mechanism that can generate a relic density for the LSP neutralino which utilizes the idea of coannihilation of the LSP with a cluster of states in the hidden sector which are degenerate in mass with the LSP. Phenomena of this type can arise in a broad class of models including extended SUGRA models with a Fayet-Iliopoulos term, models with kinetic mixings, models with the Stueckelberg mechanism, and in string and D-brane models. In many such models connector fields exist which have non-trivial gauge transformations under the hidden as well as under the visible sector gauge groups and allow for mixings of the LSP with the hidden sector gauginos and chiral fermions. The mixings between the visible and the hidden sector are typically constrained by the precision electroweak data. There are many examples of models of this type that can be constructed, but here we will consider one specific concrete manifestation as a representative of this class of models. More specifically, we will assume that there is a set of connector fields (axions) that transform non-trivially under the hidden sector  $U(1)_X^n$  gauge group (*i.e.*, the product  $U(1)_X \times U(1)_{X'} \dots$ ) as well as under the hyper-

charge gauge group  $U(1)_Y$ . In addition to the above, in the visible sector we consider a class of extended SUGRA models with nonuniversalities in the gaugino masses (see, *e.g.*, [18, 19, 20, 21] and references quoted therein) such that the gaugino masses at the scale of grand unification are of the form  $\tilde{m}_i = (1 + \delta_i)m_{1/2}$ ,  $i = 1, 2, 3$  for the gauge groups  $U(1)_Y, SU(2)_L, SU(3)_C$ . Within the above framework we discuss illustrative model points: one of these leads to an LSP which has a mixed Higgsino-wino content while the other is essentially purely wino. It is found that the model with the mixed Higgsino-wino content can produce the observed positron excess and at the same time can coannihilate with the hidden sector gauge and chiral fermions to produce a relic density consistent with the WMAP [16] constraints. In contrast, for the model where the LSP is essentially pure wino, the above phenomenon fails to bring the relic density within the reach of the WMAP data and thus a nonthermal mechanism is needed to generate the right relic density. We give now the details of the analysis.

## II. THE GENERAL $B_{\text{Co}}$ MECHANISM

As already noted in the preceding section, a fit to the PAMELA data with annihilating dark matter requires a relatively large annihilation cross section in the halo which is as much as two orders of magnitude larger (for di-boson production) than the thermal cross section needed to fit the data on the relic density of cold dark matter (CDM) consistent with WMAP. The main mechanisms discussed in the literature to reconcile the two include the enhancement of the velocity averaged annihilation cross section  $\langle\sigma v\rangle$  in the halo either by annihilation near a Breit-Wigner pole [6] or by non-perturbative enhancements (see, *e.g.*, [22, 23] and references therein).

Here we will consider an alternative mechanism consisting of a set of particles nearly degenerate in mass with the LSP but which have suppressed interactions with the visible sector states whose particle content is that of the minimal supersymmetric extension of the standard model (MSSM). When such a hidden sector is present it can act as a reservoir, significantly boosting the resulting thermal relic density of the LSP. Here we have in mind a set of hidden sector states acting as a reservoir, similar in spirit to the works of Ref. [24] (see also [25]). Additionally some states in the MSSM sector may also be degenerate in mass with the LSP. In fact for our specific models we will find that the light chargino of the MSSM will also be degenerate with the LSP. Thus, consider  $n_v$  number of sparticles in the visible sector which are essentially degenerate and  $n_h$  number of states in the hidden sector that are essentially degenerate with the neutralino LSP but have suppressed interactions relative to the MSSM interactions. In general the relic density is governed by  $\sigma_{\text{eff}} = \sum_{A,B} \sigma_{AB} \gamma_A \gamma_B$ , where the  $\gamma_A$  are the Boltzmann

suppression factors [26]

$$\gamma_A = \frac{g_A(1 + \Delta_A)^{3/2} e^{-\Delta_A x}}{\sum_B g_B(1 + \Delta_B)^{3/2} e^{-\Delta_B x}}. \quad (1)$$

Here  $g_A$  are the degrees of freedom of  $\chi_A$ ,  $x = m_{\tilde{\chi}^0}/T_x$  with  $T_x$  the temperature and  $\Delta_A = (m_{\chi_A} - m_{\tilde{\chi}^0})/m_{\tilde{\chi}^0}$ , and  $m_{\tilde{\chi}^0}$  is the mass of the LSP ( $\tilde{\chi}^0$ ). The relic abundance of dark matter at current temperatures obeys the well known proportionality  $\Omega_{\tilde{\chi}^0} h^2 \propto \left[ \int_{x_f}^{\infty} \langle\sigma_{\text{eff}} v\rangle \frac{dx}{x^2} \right]^{-1}$  where  $x_f$  is the value of  $x$  at freeze-out. Because of the small couplings of the hidden sector to the visible sector, one has  $\sigma_{\alpha\alpha}, \sigma_{\alpha\beta} \ll \sigma_{ab}$ , where  $a, b = 1, \dots, n_v$  label the MSSM sector particles that are essentially degenerate with the LSP and  $\alpha, \beta = 1, \dots, n_h$  label the hidden sector particles that are also essentially degenerate with themselves and the LSP. In this approximation one has

$$\Omega_{\tilde{\chi}^0} h^2 \simeq B_{\text{Co}} (\Omega_{\tilde{\chi}^0} h^2)_{\text{MSSM}}, \quad (2)$$

where  $(\Omega_{\tilde{\chi}^0} h^2)_{\text{MSSM}}$  is the relic density as canonically calculated using, for example, the standard tools [27] and  $\Omega_{\tilde{\chi}^0} h^2$  is the true relic density when coannihilation effects from the hidden sector are taken into account. Further,  $B_{\text{Co}}$  is the enhancement or the boost to the relic density that comes from effects of coannihilation in the hidden sector. With  $\sigma_{\alpha\alpha}, \sigma_{\alpha\beta} \ll \sigma_{ab}$ ,  $B_{\text{Co}}$  is then given by

$$\begin{aligned} B_{\text{Co}} &\simeq \frac{\sum_{a,b} \int_{x_f}^{\infty} \langle\sigma_{ab} v\rangle \gamma_a \gamma_b \frac{dx}{x^2}}{\sum_{a,b} \int_{x_f}^{\infty} \langle\sigma_{ab} v\rangle \tilde{\gamma}_a \tilde{\gamma}_b \frac{dx}{x^2}}, \\ \gamma_a &= \frac{g_a(1 + \Delta_a)^{3/2} e^{-\Delta_a x}}{\sum_b g_b(1 + \Delta_b)^{3/2} e^{-\Delta_b x}}, \\ \tilde{\gamma}_a &= \frac{g_a(1 + \Delta_a)^{3/2} e^{-\Delta_a x}}{\sum_A g_A(1 + \Delta_A)^{3/2} e^{-\Delta_A x}}. \end{aligned} \quad (3)$$

Here  $A$  runs over channels which coannihilate both in the MSSM sector and in the hidden sector (*i.e.*,  $A = 1, \dots, n_v + n_h$ ) and  $g_A$  are the degrees of freedom for particle  $A$ ; for example,  $g = 2$  for a neutralino and  $g = 4$  for a chargino. In the limit that  $(\sigma v)_{ab}$  are independent of  $a, b$  and all  $\Delta_A$  nearly vanish, we find the simple relation

$$B_{\text{Co}} \simeq \left(1 + \frac{d_h}{d_v}\right)^2. \quad (4)$$

Here  $d_h = \sum_{\alpha} g_{\alpha}$  is the number of degrees of freedom for the coannihilating channels in the hidden sector (with suppressed cross sections in the coannihilation process) and  $d_v$  is the number of degrees of freedom in the MSSM sector for the coannihilating channels which contribute to the coannihilations with the LSP and have interactions of normal strength. For the  $U(1)$  hidden sector model with each  $U(1)$  providing two Majorana states with the chargino coannihilating with the LSP, under conditions of essentially complete degeneracy of the chargino and the

LSP<sup>1</sup>,  $B_{C_0} = (1 + \frac{2}{3}n)^2$ , while as this degeneracy becomes lifted, the maximal value is  $B_{C_0} = (1 + 2n)^2$ .

### III. SUSY MODELS WITH ENHANCEMENT OF THE THERMAL RELIC DENSITY VIA $B_{C_0}$

As noted above a  $B_{C_0}$  of the type discussed in Eq. (4) can be obtained in a class of models where the hidden sector has suppressed interactions with the visible sector. Below we construct one explicit example where a hidden sector with an extended  $U(1)^n$  gauge symmetry couples with the MSSM sector via the hypercharge gauge field. Specifically, we consider an additional contribution to the MSSM to be of the form [28], [24]

$$\Delta\mathcal{L} = \int d^2\theta d^2\bar{\theta} \sum_{m=1}^{N_S} \left[ \sum_{l=1}^{N_V} M_{l,m} V_l + (\Phi_m + \bar{\Phi}_m) \right]^2, \quad (5)$$

where  $V = \{B, X, X', X'' \dots\}$  are vector supermultiplets which include the hypercharge gauge multiplet  $B$ , and  $\Phi_m$  are a collection of chiral supermultiplets and  $(N_S, N_V > N_S)$  are the number of (axions, vectors).

Thus for the  $U(1)^n$  extended models we consider  $N_S = n$  and  $N_V = n + 1$  such that  $N_S$  number of vector bosons absorb  $N_S$  number of axions leading to  $N_S$  number of massive  $Z'$  bosons [28, 29]. A full analysis would include also the electroweak symmetry breaking from the MSSM sector generating a mixing between the hidden and the visible sectors. Models of this type can arise in a very broad class of theories including extensions of the SM, extended supergravity models, and in strings and in D-brane models. Specifically we will be interested in an extension of supergravity models with the hidden sector gauge group  $U(1)_X^n$  with mixings between the visible and the hidden sector given by Eq.(5). This extension then leads to a  $(4 + 2n) \times (4 + 2n)$  dimensional neutralino mass matrix of the form

$$\mathcal{M}^{[1/2]} = \left( \begin{array}{c|c} [\mathbf{M}_1]_{2n \times 2n} & [\mathbf{M}_2]_{2n \times 4} \\ \hline [\mathbf{M}_2]_{4 \times 2n}^T & [\mathbf{S}]_{4 \times 4} \end{array} \right), \quad (6)$$

where

$$\mathbf{S}_{4 \times 4} = \begin{pmatrix} \tilde{m}_1 & 0 & \alpha & \beta \\ 0 & \tilde{m}_2 & \gamma & \delta \\ \alpha & \gamma & 0 & -\mu \\ \beta & \delta & -\mu & 0 \end{pmatrix}, \quad (7)$$

and where  $\alpha = -c_\beta s_W M_Z$ ,  $\beta = s_\beta s_W M_Z$ ,  $\gamma = c_\beta c_W M_Z$ ,  $\delta = -s_\beta c_W M_Z$ . Here  $(s_\beta, c_\beta) = (\sin \beta, \cos \beta)$ , where  $\tan \beta = \langle H_2 \rangle / \langle H_1 \rangle$  and  $\langle H_2 \rangle$  gives mass to the up quarks and  $\langle H_1 \rangle$  gives mass to the down quarks and the leptons, and  $(s_W, c_W) = (\sin \theta_W, \cos \theta_W)$ , where  $\theta_W$  is the weak angle. The remaining quantities in Eq.(6) are

$$[\mathbf{M}_1]_{2n \times 2n} = \begin{pmatrix} M_1^{(n)} \hat{U} & \hat{O} & \dots & \hat{O} \\ \hat{O} & M_1^{(n-1)} \hat{U} & & \hat{O} \\ \vdots & & \ddots & \vdots \\ \hat{O} & \hat{O} & \dots & M_1^{(1)} \hat{U} \end{pmatrix} \quad (8)$$

and

$$[\mathbf{M}_2]_{2n \times 4} = \begin{pmatrix} M_2^{(n)} \hat{P} & \hat{O} \\ M_2^{(n-1)} \hat{P} & \hat{O} \\ \vdots & \vdots \\ M_2^{(1)} \hat{P} & \hat{O} \end{pmatrix}, \quad (9)$$

where the ellipses indicate additional  $U(1)$ s and where

$$\hat{U} = \begin{pmatrix} 0 & 1 \\ 1 & 0 \end{pmatrix}, \quad \hat{P} = \begin{pmatrix} 1 & 0 \\ 0 & 0 \end{pmatrix}, \quad \hat{O} = \begin{pmatrix} 0 & 0 \\ 0 & 0 \end{pmatrix}. \quad (10)$$

The  $4 \times 4$  dimensional matrix of Eq.(7) is the neutralino mass matrix in the MSSM sector, the  $(2n) \times (2n)$  dimensional mass matrix of Eq.(8) is the neutralino mass matrix in the hidden sector, and the  $2n \times 4$  dimensional matrix of Eq.(9) is the matrix of off-diagonal terms which produce the mixings between the hidden sector and the MSSM sector. These mixings are controlled by the ratios  $\epsilon \equiv M_2/M_1$ , etc. all of which we assume to be much smaller than unity [29]. We also assume that the hidden sector neutralinos are all essentially degenerate with the LSP neutralino. Thus in the diagonal basis we have the set of neutralino states  $\tilde{\chi}_i^0$  ( $i = 1, \dots, 4 + 2n$ ) where the last  $n_h \equiv 2n$  are the set of neutralinos from the hidden sector. The above serves as an illustrative example, but our analysis would apply to any class of models which satisfy the conditions discussed in the beginning of this section.

We discuss now two specific model points which fit the PAMELA data but lead to significantly different sparticle spectra and signatures in the direct detection of dark matter and at colliders.

#### Higgsino-wino model (HWM)

Here the soft nonuniversal SUGRA parameters are

$$(m_0, m_{1/2}, A_0) = (800, 558, 0) \text{ GeV}, \quad \tan \beta = 5, \\ \text{sign}(\mu) = +, \quad \delta_{1,2,3} = (-.09, -.50, -.51), \quad (11)$$

and the gaugino-Higgsino content of the LSP is  $\tilde{\chi}^0 = 0.726\lambda_B - 0.616\lambda_W + 0.260\tilde{h}_1 - 0.160\tilde{h}_2 + C_h \Delta \tilde{\chi}_h^0$ . Thus the LSP has a strong Higgsino component in addition to strong wino and bino components. Nevertheless

<sup>1</sup> This value of  $B_{C_0}$  is the asymptotic limit when there is a complete degeneracy of the matter in the hidden sector and of the chargino with the LSP. There is also an upper asymptotic limit which corresponds to a complete split of the chargino from the LSP which gives  $B_{C_0} = (1 + 2n)^2$ , so as the chargino moves from a complete degeneracy with the LSP to a complete split, one goes from  $(1 + \frac{2}{3}n)^2 \rightarrow (1 + 2n)^2$ . For  $n = 3$  the above corresponds to the transition:  $B_{C_0} = 9 \rightarrow B_{C_0} = 49$ .

we will refer to this model as the Higgsino-wino model (HWM) because these components play a major role in the analysis to follow. The quantity  $C_h \Delta \tilde{\chi}_h^0$  is the component in the hidden sector and is found by explicit calculation to be rather small ( $|C_h| < 1\%$  for  $n = 3$ ).

#### Pure wino model (PWM)

Here the soft parameters are

$$(m_0, m_{1/2}, A_0) = (1000, 850, 0) \text{ GeV}, \tan \beta = 10, \\ \text{sign}(\mu) = +, \delta_{1,2,3} = (0, -0.7, 0), \quad (12)$$

and the gaugino-Higgsino content of the LSP is  $\tilde{\chi}^0 = 0.009\lambda_B - 0.996\lambda_W + 0.081\tilde{h}_1 - 0.023\tilde{h}_2 + C_h \Delta \tilde{\chi}_h^0$ . In this model the LSP is dominated by the wino component and thus this model will be referred to as the (essentially) pure wino model (PWM), while the component in the hidden sector  $C_h \Delta \tilde{\chi}_h^0$  is still small (i.e., also  $|C_h| < 1\%$ , for  $n = 3$ ).

For both model points given above one finds the following mass relations

$$m_{\tilde{\chi}^\pm} \simeq m_{\tilde{\chi}^0}, \quad m_{\tilde{\chi}_2^\pm} \simeq m_{\tilde{\chi}_3^0} \simeq m_{\tilde{\chi}_4^0}. \quad (13)$$

These mass relations follow simply from the condition that  $\tilde{m}_2 < \tilde{m}_1$ ,  $|\mu| \gg M_Z$ . However, a distinguishing feature of the HWM is that the mass gap between the LSP and the chargino is order  $\sim 10$  GeV while for the case of the PWM the mass gap is order the pion mass. The neutralino annihilation in both models is dominated by  $W^+W^-$  production in the halo. We will discuss this in much more detail in what follows.

#### IV. THE PAMELA POSITRON DATA AND THERMAL NEUTRALINO DARK MATTER

One issue of interest in this work is to address the compatibility of the recent PAMELA positron data and the WMAP data. Thus, we begin with a brief review of the calculation of the primary positron flux relevant for the models considered here.

The positron flux which enters as a solution to the diffusion loss equation under steady state conditions is given by [30],[31],[3]

$$\Phi_{\bar{e}}(E) = \frac{B_{\bar{e}} v_{\bar{e}}}{8\pi b(E)} \frac{\rho_{\odot}^2}{m_{\tilde{\chi}^0}^2} F(E), \quad (14)$$

$$F(E) = \int_E^{M_{\tilde{\chi}^0}} dE' \sum_k \langle \sigma v \rangle_{\text{halo}}^k \frac{dN_{\bar{e}}^k}{dE'} \cdot \mathcal{I}(E, E'). \quad (15)$$

In the above,  $B_{\bar{e}}$  is a so-called boost factor which parameterizes the possible local inhomogeneities of the dark matter distribution. Large boost factors have been used in the literature, even as large as 10,000, to explain the PAMELA data. However, we will show that

there are various cases where boost factors in the range  $\sim (1 - 5)$  fit the PAMELA data in models of supersymmetry (SUSY). In Eq. (14)  $v_{\bar{e}}$  is the positron velocity,  $v_{\bar{e}} \sim c$ ,  $\rho_{\odot} = \rho(r_{\odot})$  is the local dark matter density in the halo (with  $r_{\odot} \sim 8.5$  kpc) and  $\rho_{\odot}$  lies in the range  $(0.2 - 0.7)$  GeV/cm<sup>3</sup> [32]. Further,  $b(E)$  in Eq.(14) is given by  $b(E) = E_0(E/E_0)^2/\tau_E$ , with  $E$  in GeV and  $E_0 \equiv 1$  GeV, and where  $\tau_E = \tau 10^{16}$  s, where  $\tau$  values as large (1-5) have been considered in the literature and we adopt  $\tau = 3$  [33]. Here  $\langle \sigma v \rangle_{\text{halo}}$  is the velocity averaged cross section in the halo of the galaxy and  $\mathcal{I}(E, E')$  is the halo function. We have considered both the Navarro, Frenk and White (NFW) and Moore et. al [34] profiles coupled with various diffusion models. The diffusion loss equation depends on the propagation parameters  $\delta$ ,  $K_0$  solved in the region modeled with cylindrical symmetry bounding the galactic plane with height  $2L$ . The dimensionless halo function has been parameterized to satisfy constraints on the boron to carbon ratio [3, 31] such that

$$\mathcal{I}(E, E') = a_0 + a_1 \tanh\left(\frac{b_1 - \ell}{c_1}\right) \times \left[ a_2 \exp\left(-\frac{(\ell - b_2)^2}{c_2}\right) + a_3 \right] \quad (16)$$

and where  $\ell = \log_{10} \lambda_D$  with  $\lambda_D$  in units of kpc

$$\lambda_D(E, E') = 2\sqrt{K_0 \tau_E D^{-1} (E^{-D} - E'^{-D})} \quad (17)$$

$$D = 1 - \delta. \quad (18)$$

Model	$\delta$	$K_0$ (kpc <sup>2</sup> /Myr)	$L$ (kpc)	
MIN(M2)	0.55	0.00595	1	
Halo model propagation	$a_0$	$a_1$	$a_2$	$a_3$
NFW MIN(M2)	0.500	0.774	-0.448	0.649
Halo function coeff.	$b_1$	$b_2$	$c_1$	$c_2$
	0.096	192.8	0.211	33.88
$w_0^{\bar{e}}$	$w_1^{\bar{e}}$	$w_2^{\bar{e}}$	$w_3^{\bar{e}}$	
- 2.28838	-0.605364	- 0.287614	-0.762714	
$w_4^{\bar{e}}$	$w_5^{\bar{e}}$	$w_6^{\bar{e}}$	$w_7^{\bar{e}}$	
- 0.319561	-0.0583274	- 0.00503555	-0.00016691	

TABLE I: The class of models consistent with the boron/carbon ratio [31] considered here. The MED and MAX halo models are not shown since they tend to overproduce the positron flux at low energies. Also shown are the coefficients ( $a_i, b_i$ ) entering in the dimensionless halo function for positron propagation [3] where the NFW profile is used and the MIN(M2) diffusion parameters enter. The last set of entries are the fragmentation coefficients  $w_i^{\bar{e}}$  for the  $W^+W^-$  mode [30].

For the case of dark matter in the halo which primarily annihilates into  $W$  boson pairs, the positron fragmenta-



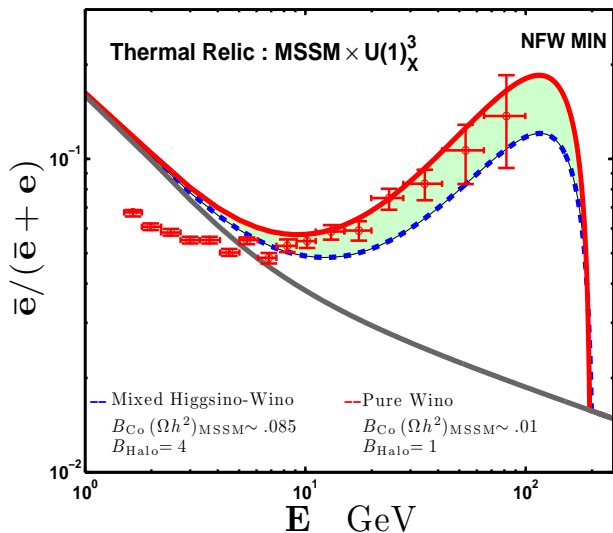


FIG. 1: SUSY predictions for the positron flux ratio: The top curve is for the PWM (see Eq. (12)) where the neutralino is wino dominated, with  $m_{\tilde{\chi}^0} = 199$  GeV, and  $\langle\sigma v\rangle_{WW} = 1.96 \times 10^{-24} \text{ cm}^3/\text{s}$  with a  $B_{\text{clump}}$  of 1.0 and  $\Omega h^2 \sim .01$  with a  $B_{Co} \sim 9$  (the asymptotic value for the wino case). The middle curve is for the HWM (see Eq. (11)) where the neutralino has a mixed wino, bino and Higgsino content, with  $m_{\tilde{\chi}^0} = 195$  GeV, and  $\langle\sigma v\rangle_{WW} = 0.28 \times 10^{-24} \text{ cm}^3/\text{s}$  with  $B_{\text{clump}}$  of 4 and gives rise to an  $\Omega h^2 = .085$ , with a  $B_{Co}$  of 16. We have taken  $\rho_{\odot} = 0.6 \text{ GeV}/\text{cm}^3$  and  $\tau = 3$  for both curves. Slightly larger clump factors can easily accommodate a downward shift in the product  $\rho_{\odot}^2 \tau E$ . The bottom curve is the background. The experimental data is from [1].

tion function can be expressed as [30]

$$\frac{dN_{\bar{e}}^{WW}}{dx} = \exp \left[ \sum_n w_n^{\bar{e}} (\ln(x))^n \right], \quad (19)$$

where  $x = E/m$  and the fragmentation function was fit in the analysis of [30] with HERWIG [35].

The positron fluxes in the absence of dark matter annihilations have been parameterized in [36] using fits to the analysis which we adopt here. For the case of positrons annihilating strongly into  $W$  bosons, we find that the MED and MAX models with NFW or Moore profile tend to overproduce the positron flux data at energies well above the region of solar modulation. Thus the class of models we consider restricts the profile/diffusion model to a MIN(M2) scenario, at least for the case of positrons. We thus display only the fit parameters for this scenario in Table (I). The fit parameters for the halo function are also shown in Table (I) along with the fragmentation functions for dark matter annihilations into  $W^+W^-$  states. As discussed in the previous section, in the analysis here we fix the soft parameters of the SUGRA models at the scale of grand unification and examine the implications of the model at the electroweak scale. The analysis shows that the mixed Higgsino-wino model (HWM) can

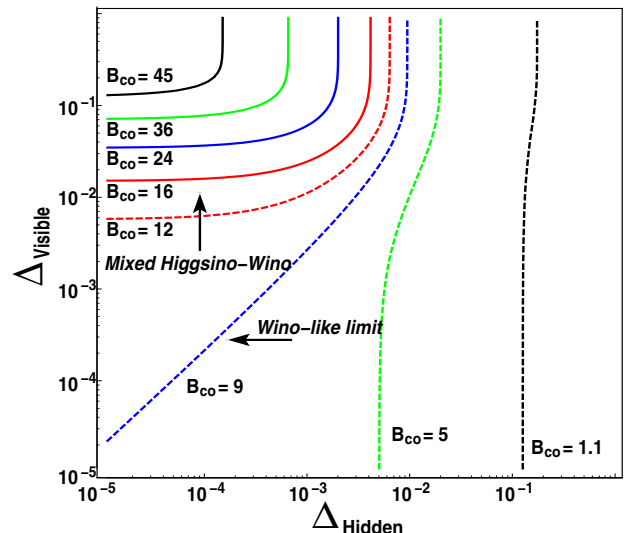


FIG. 2: An illustration of the  $B_{Co}$ -mechanism with a contour plot of constant  $B_{Co}$  in the  $\Delta_{\text{Visible}}$  vs  $\Delta_{\text{Hidden}}$  plane for the  $U(1)^3$  extended SUGRA model. Large values of  $B_{Co}$  are admissible for the mixed Higgsino-wino case (see the text). The region to the right of the contour  $B_{Co} = 9$  is the domain of the PWM while the region to the left of it is the domain of the HWM. Thus the largest value of  $B_{Co}$  in the PWM is 9 while for the HWM case  $B_{Co}$  can be significantly larger.

have mass splittings between the LSP and the chargino of around 10 GeV and still produce relatively large halo cross sections that do not require large boost factors to fit the PAMELA data. On the other hand for the pure (or nearly pure) wino LSP one finds that the mass splitting of the LSP neutralino and the light chargino is negligibly small and this result is generally a necessary consequence of the wino dominated class of models. A numerical analysis of the positron excess for comparison with the PAMELA experiment is presented in Fig. (1) for the HWM and for the PWM. It is found that both models are capable of fitting the PAMELA data. A wino LSP of a mass near 200 GeV has been suggested in Ref. [4] as a good candidate for explaining the positron excess using a methodology and choice of parameters similar to the ones used here, though the model in that study and this study are quite different.

While both the HWM and PWM are successful at reproducing the PAMELA positron excess, the thermal relic densities for the two models are very different. For the case of the HWM, the relic density can be consistent with the WMAP data for a thermal LSP. However, the relic density for the PWM from thermal processes is at best about a factor of 10 too small and here one needs a non-thermal mechanism to be compatible with WMAP, as was assumed in the work of Ref. [4]. The compatibility of the relic density with WMAP for the HWM comes about because of the enhancement from the hidden sector, *i.e.*, because of the  $B_{Co}$  factor. As seen in Fig.(2),  $B_{Co}$  can acquire values as large as 45. This limiting value

Model	$\delta$	$K_0$ (kpc <sup>2</sup> /Myr)	$L$ (kpc)	$V_{\text{conv}}$ (km/s)
MIN	0.85	0.0016	1	13.5
MED	0.70	0.0112	4	12
MAX	0.46	0.0765	15	5

TABLE II: Specific models considered here, consistent with the boron/carbon ratio [38]

of  $B_{\text{Co}}$  is realized only when there is a complete split between the LSP and the light chargino. While this value is not achieved in the HWM, the presence of a  $\sim 10$  GeV split between the LSP and the chargino does conspire to produce a  $B_{\text{Co}}$  in the range 16 – 20 while for the PWM the maximal value one may have is  $B_{\text{Co}} \sim 9$ . While a factor of 16 – 20 is good enough to boost the relic density for the HWM to be consistent with WMAP, for the PWM the relic density still falls below the WMAP corridor and would require a very large collection of degenerate states (e.g.,  $n = 11$ ) to bring the relic density within the corridor.

## V. ANALYSIS OF THE $\bar{p}$ FLUX

Quite similar to the analysis of the positron flux, the anti-proton flux assumes a steady state solution to a diffusion equation, retaining a factorized form split between the particle physics content and the astrophysical details, the latter encoding the halo and the propagation model. Thus the anti-proton flux from annihilating neutralinos in the galaxy is given by [37]

$$\Phi_{\bar{p}}(T) = B_{\bar{p}} \frac{v_{\bar{p}}}{8\pi} \frac{\rho_{\odot}^2}{m_{\tilde{\chi}^0}^2} R(T) \sum_k \langle \sigma v \rangle_{\text{halo}}^k \frac{dN_{\bar{p}}^k}{dT} \quad (20)$$

where  $T$  is the kinetic energy, and  $R(T)$  has been fit as in Ref. [3] for various profile/diffusion models. Specifically for the NFW models one has

$$\begin{aligned} \text{MIN} : \log_{10} [R(T)/\text{Myr}] &= 0.913 + 0.601 r \\ &\quad - 0.309 r^2 - 0.036 r^3 + 0.0122 r^4 \\ \text{MED} : \log_{10} [R(T)/\text{Myr}] &= 1.860 + 0.517 r \\ &\quad - 0.293 r^2 - 0.0089 r^3 + 0.0070 r^4 \\ \text{MAX} : \log_{10} [R(T)/\text{Myr}] &= 2.740 - 0.127 r \\ &\quad - 0.113 r^2 + 0.0169 r^3 - 0.0009 r^4, \end{aligned} \quad (21)$$

where  $r = r(T) = \log_{10}(T/\text{GeV})$ , and where the  $\bar{p}$  propagation parameters are given in Table (II).

As discussed already, for the models of interest we study here, the contribution to  $\langle \sigma v \rangle$  in the halo is dominated by several orders of magnitude from the annihilations of neutralino dark matter into  $W^+W^-$  bosons. The  $\bar{p}$  fragmentation functions needed for the analysis of the flux are given by [39],[30] as

$$\frac{dN_{\bar{p}}^{WW}}{dx} = (p_1 x^{p_3} + p_2 |\log_{10} x|^{p_4})^{-1}, \quad (22)$$

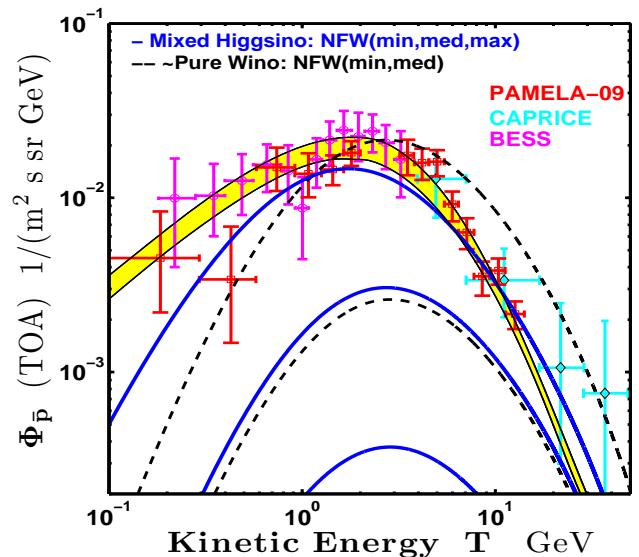


FIG. 3: The absolute anti-proton flux for the HWM with various halo/diffusion models NFW(MIN,MED,MAX) and only (MIN,MED) for the PWM. Here  $\rho_{\odot} = 0.3$  GeV/cm<sup>3</sup> (the signal scales as  $\rho^2$ ),  $B_{\bar{p}} = 1$ . For the background flux (band) we have adopted the parameterizations of Ref. [40]. Also shown is the preliminary PAMELA data [41, 42] along with the earlier data sets from BESS and CAPRICE [43]. The analysis here shows that the models discussed in this work can accommodate the anti-proton flux constraints.

where here  $x = T/m_{\tilde{\chi}^0}$  and  $T$  is the kinetic energy. The parameters  $p_i$  in the above equation depend on the neutralino mass and are given by

$$p_i(m) = (a_{i1} m^{a_{i2}} + a_{i3} m^{a_{i4}})^{-1}, \quad m = m_{\tilde{\chi}^0}, \quad (23)$$

where the values of  $a_{ij}$  are given in Table (III).

	$j = 1$	$j = 2$	$j = 3$	$j = 4$
$i = 1$	306.0	0.28	$7.2 \times 10^{-4}$	2.25
$i = 2$	2.32	0.05	0	0
$i = 3$	-8.5	-0.31	0	0
$i = 4$	-0.39	-0.17	$-2.0 \times 10^{-2}$	0.23

TABLE III: Coefficients  $a_{ij}$  for  $W^+W^-$  process entering into the anti-proton fragmentation functions [39][30].

The anti-proton flux observed at the top of the atmosphere including solar modulation can be accounted for by replacing  $\Phi_{\bar{p}}(T) = \Phi_{\bar{p}}(T, \phi_F) = \Phi_{\bar{p}}(T + |Z|\phi_F)$  and including a kinetic energy correction ratio, such that

$$\Phi_{\bar{p}}^{\oplus}(T) = \frac{((T + m_p)^2 - m_p^2) \cdot \Phi_{\bar{p}}(T + |Z|\phi_F)}{(T + |Z|\phi_F + m_p)^2 - m_p^2} \quad (24)$$

where  $m_p$  is the proton mass,  $Z = 1$ , and the Fisk potential  $\phi_F$  is taken as 500 MV. In Fig.(3) we give an analysis of the anti-proton flux with the parameters indicated in the caption of the figure showing both the

SUSY signal and the backgrounds. The analysis demonstrates that HWM is only currently constrained for the MAX diffusion model, while the PWM is constrained for a MED diffusion model but is essentially unconstrained for a MIN diffusion model. Similar conclusions regarding the sensitivity of the  $\bar{p}$  flux to the halo/diffusion model have also been made in the first Ref. of [6].

In summary, the findings here for the PWM are generally in good agreement with the recent results of [4], and further we find that the HWM is only very weakly constrained by the PAMELA anti-proton data as well as by the earlier BESS and CAPRICE data.

## VI. PHOTON FLUX; EGRET AND FERMI-LAT

The continuum photon source from the annihilating SUSY dark matter is given by [44]

$$\frac{d^2\Phi_\gamma}{d\Omega dE} = \frac{1}{2} \frac{r_\odot \rho_\odot^2}{4\pi m_{\tilde{\chi}^0}^2} \sum_k \langle\sigma v\rangle_{\text{halo}}^k \frac{dN_\gamma^k}{dE} J(\psi). \quad (25)$$

where  $J(\psi) = (r_\odot \rho_\odot^2)^{-1} \int_0^\infty \rho^2(r) dl(\psi)$  and  $r^2 = l^2 + r_\odot^2 - 2lr_\odot \cos\psi$  with  $\psi$  the angle of integration over the line of sight. After integration, the astrophysics is encoded in  $\bar{J} \cdot \Delta\Omega$ , where  $\bar{J} = (1/\Delta\Omega) \int_{\Delta\Omega} J(\psi) d\Omega$  and various values of  $\bar{J}$  are given for a collection of angular maps, in, for example [45] (see also [46, 47],[48] for early work). As remarked previously,  $W$  boson pair production is the dominant contributor to the photon flux in the models we discuss, and an upgraded set of fragmentation functions are given in [3] and are shown below

$$E \frac{dN_\gamma}{dE} = \exp \left[ \sum_n \frac{w_n^\gamma}{n!} \ln^n(E/M) \right]. \quad (26)$$

Separately, effects due to Brehmstrahlung have been studied in Ref. [49] and are easily accounted for. Values of  $w_n^\gamma$  relevant for the analysis are listed below.

$w_0^\gamma$	$w_1^\gamma$	$w_2^\gamma$	$w_3^\gamma$	$w_4^\gamma$	$w_5^\gamma$	$w_6^\gamma$
-6.751	-5.741	-3.514	-1.964	-0.8783	-0.2512	-0.03369

Our result for the photon flux is given in Figure (4) where we exhibit the gamma ray flux arising from the annihilation of neutralino dark matter in the 10 – 20 region ( $10 \text{ deg} < |b| < 20 \text{ deg}$ ), ( $0 \text{ deg} < l < 360 \text{ deg}$ ) [latitude  $b$  and longitude  $l$ ] which is the region relevant for comparison with the preliminary FERMI-LAT results [52]. Figure (4) shows that the more accurate FERMI-LAT data falls in magnitude below the EGRET data. Our analysis of the photon flux for the HWM is consistent with the FERMI-LAT and EGRET data, while the PWM may show an excess at extended energy ranges. Note the maximum of the flux for the signal appears at the last data point of the FERMI data near 10 GeV.

We note that monochromatic sources [53] (calculated with DarkSusy [27]) yield a further distinguishing feature

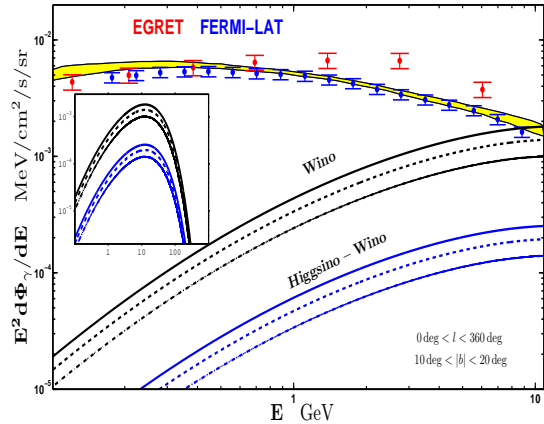


FIG. 4: An exhibition of the gamma ray flux the HWM and the PWM in the coordinate range indicated, with the Einasto, NFW, and Isothermal profiles with the same halo cross sections as given in Figs.(1,3). Shown are the EGRET [50] results and FERMI-LAT results as reported in [51, 52] along with the background flux (band). The analysis here shows that both models can accommodate the photon flux constraint.

between the HWM and the PWM. Here the PWM will produce a significantly stronger monochromatic source than the HWM which is dictated by the size of the relative cross sections since  $m_{\tilde{\chi}^0}$  are essentially the same for the HWM and PWM:

$$\text{HWM} : \langle\sigma v\rangle_{\gamma\gamma}^{1\text{-loop}} = 1.6 \times 10^{-28} \text{ cm}^3/\text{s}, \quad (27)$$

$$\text{PWM} : \langle\sigma v\rangle_{\gamma\gamma}^{1\text{-loop}} = 2.0 \times 10^{-27} \text{ cm}^3/\text{s}.$$

$$\text{HWM} : \langle\sigma v\rangle_{\gamma Z}^{1\text{-loop}} = 1.0 \times 10^{-27} \text{ cm}^3/\text{s}, \quad (28)$$

$$\text{PWM} : \langle\sigma v\rangle_{\gamma Z}^{1\text{-loop}} = 1.3 \times 10^{-26} \text{ cm}^3/\text{s}.$$

Thus while the photon energies will be essentially the same ( $m_{\tilde{\chi}^0}$  for the  $\gamma\gamma$  channel and  $m_{\tilde{\chi}^0}(1-\delta)$ ,  $\delta = M_Z^2/(2m_{\tilde{\chi}^0})^2$  for the  $\gamma Z$  channel) in fact, the PWM would predict a flux an order of magnitude larger than the HWM in both channels.

## VII. EFFECTS ON DIRECT DETECTION

The direct detection of dark matter is sensitive to the Higgsino content of the LSP. For the HWM the LSP has a significant Higgsino component and thus the spin independent cross section for neutralino-proton scattering in the direct detection dark matter experiments is significant and may lie within reach of the next generation experiments. For the PWM, we remind the reader that the LSP is essentially 100% wino, and in this case the spin independent cross section will be very small, essentially beyond the limit of sensitivity of near future experiments on the direct detection of dark matter. Specifically, a direct calculation using MicrOmegas (see Ref. 2 of [27])

yields a neutralino-proton cross section of

$$\text{HWM} : \sigma_{\tilde{\chi}_0^0 p}^{\text{SI}} = 6.62 \times 10^{-8} \text{ pb}, \quad (29)$$

$$\text{PWM} : \sigma_{\tilde{\chi}_0^0 p}^{\text{SI}} = 1.15 \times 10^{-9} \text{ pb}, \quad (30)$$

which translates into a recoil rate on germanium targets of

$$\text{HWM} : R = 1.58 \times 10^{-2} / \text{day/kg}, \quad (31)$$

$$\text{PWM} : R = 2.81 \times 10^{-4} / \text{day/kg}, \quad (32)$$

and on liquid xenon targets of

$$\text{HWM} : R = 2.60 \times 10^{-2} / \text{day/kg}, \quad (33)$$

$$\text{PWM} : R = 4.63 \times 10^{-4} / \text{day/kg}, \quad (34)$$

when integrated over the entire range of nuclear recoil energies. For the pure wino and pure higgsino cases the cross sections can receive important loop corrections[55]. From the analysis of [55] one can estimate these effects, and they are found not be significant for the parameter space we investigate. Clearly, the prospects for the direct detection of the relic LSP are most promising for the HWM, which should be accessible in near future dark matter experiments with an improvement in sensitivity by a small factor, as is expected to occur. For the PWM the observation of the spin independent cross section requires an improvement in sensitivity by a factor of about 100 which is unlikely to happen in the foreseeable future.

### VIII. COLLIDER IMPLICATIONS OF PAMELA INSPIRED MODELS

*Discovery Modes at the LHC:* An important and robust aspect of supersymmetric models which are capable of generating the observed PAMELA positron excess is that some superpartners will necessarily be light and are therefore potentially discoverable at the LHC. Certain key physical masses for the HWM and PWM are given in Table (IV). All masses are computed from the high-scale

Mass	HWM	PWM	Mass	HWM	PWM
$m_{\tilde{\chi}_0^0}$	198.9	195.2	$m_{\tilde{t}_1}$	648.5	1516
$m_{\tilde{\chi}_2^0}$	217.0	357.0	$m_{\tilde{t}_2}$	866.8	1749
$m_{\tilde{\chi}_3^0}$	429.9	1025	$m_{\tilde{b}_1}$	841.4	1729
$m_{\tilde{\chi}_4^0}$	451.3	1029	$m_{\tilde{b}_2}$	970.2	1902
$m_{\tilde{\chi}_1^\pm}$	208.8	195.5	$m_{\tilde{\tau}_1}$	817.7	1011
$m_{\tilde{\chi}_2^\pm}$	448.6	1036	$m_{\tilde{\tau}_2}$	822.8	1041
$m_{\tilde{g}}$	707.1	1929			

TABLE IV: Relevant SUSY mass spectra for the HWM and PWM as calculated from the high-scale boundary conditions given in (11) and (12), respectively. All masses are in GeV.

boundary conditions of Eq.(11) and Eq.(12) after renormalization group evolution using SoftSUSY [54]. One finds that for the PWM the sum rules of Eq.(13) are satisfied with an accuracy of less than 0.5%. In fact, for the PWM there is an almost perfect degeneracy between the lightest chargino and the lightest neutralino mass, as is typical for models with a wino-dominated LSP. In the HWM this mass difference is larger, reflecting the larger proportion of bino and Higgsino components for the LSP wave function, so that Eq.(13) is satisfied only at the 5-6% level. But as we saw in Section IV this results in a larger  $B_{C_0}$  factor for the HWM.

One may note that in Table (IV) a significant difference in mass scales for the  $SU(3)$ -charged superpartners of the HWM and of the PWM. This difference in the mass scales has large implications for the discovery prospects of the two models. To analyze the signatures of these models at the LHC we generated events using PYTHIA followed by a detector simulation using PGS4 [56]. Two data sets for each model at  $\sqrt{s} = 14$  TeV were generated for  $10 \text{ fb}^{-1}$  and  $100 \text{ fb}^{-1}$  of signal events, as well as a  $500 \text{ pb}^{-1}$  sample at  $\sqrt{s} = 10$  TeV for each model. In addition we considered a suitably-weighted sample of  $5 \text{ fb}^{-1}$  Standard Model background events, consisting of Drell-Yan, QCD dijet,  $t\bar{t}$ ,  $b\bar{b}$ ,  $W/Z$ +jets and diboson production. Events were analyzed using level one (L1) triggers in PGS4, designed to mimic the CMS trigger tables [57]. Object-level post-trigger cuts were also imposed. We require all photons, electrons, muons and taus to have transverse momentum  $p_T \geq 10$  GeV and  $|\eta| < 2.4$  and we require hadronic jets to satisfy  $|\eta| < 3$ . Additional post-trigger level cuts were implemented for specific analyses, as described below.

We begin with standard SUSY discovery modes [58], slightly modified to maximize the signal significance for these models. These five signatures are collected in Table (V) for  $10 \text{ fb}^{-1}$  of integrated luminosity. In all cases we require transverse sphericity  $S_T \geq 0.2$  and at least 250 GeV of  $\cancel{E}_T$  except for the trilepton signature, where we place a cut of  $\cancel{E}_T \geq 200$  GeV. The multijet channel includes a veto on isolated leptons and requires at

Signature	HWM		PWM	
	Events	$S/\sqrt{B}$	Events	$S/\sqrt{B}$
Multijets	8766	183.74	50	1.05
Lepton + jets	2450	32.25	26	0.34
OS dileptons + jets	110	6.39	4	0.23
SS dileptons + jets	60	11.77	0	NA
Trileptons + jets	14	2.47	0	NA

TABLE V: LHC discovery channels for the HWM and the PWM: Event counts are after  $10 \text{ fb}^{-1}$  of integrated luminosity. All signatures require transverse sphericity  $S_T \geq 0.2$  and at least 250 GeV of  $\cancel{E}_T$  except for the trilepton signature, where only  $\cancel{E}_T \geq 200$  GeV is required. Here (OS,SS) = (opposite sign, same sign)



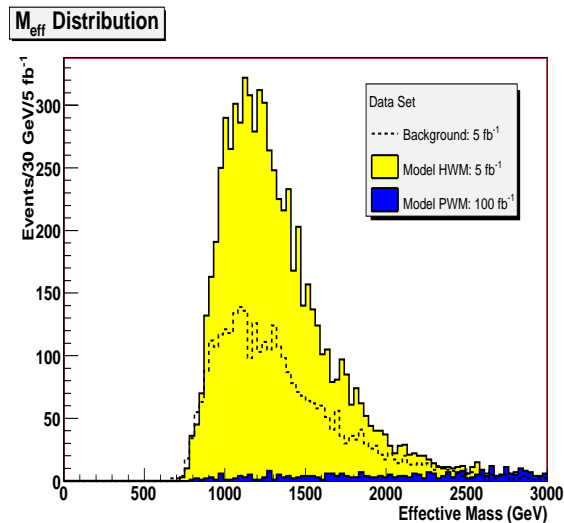


FIG. 5: Effective mass distribution for the Higgsino-wino mixed model(HWM) for  $5 \text{ fb}^{-1}$  (yellow) and the wino model for  $100 \text{ fb}^{-1}$  (blue) along with the Standard Model background (dashed open histogram).

least four jets with the transverse momenta of the four leading jets satisfying  $p_T \geq (200, 150, 50, 50)$  GeV, respectively. For the leptonic signatures we include only  $e^\pm$  and  $\mu^\pm$  final states and demand at least two jets with the leading jets satisfying  $p_T \geq (100, 50)$  GeV, respectively. For the case of the HWM, the existence of light squarks and gluinos give rise to a relatively large number of events passing the cuts, and thus the model is easily accessible at the LHC in almost all channels. In fact, we find that this particular model point gives rise to  $\sim 150$  multijet events with  $\cancel{E}_T \geq 250$  GeV with just  $500 \text{ pb}^{-1}$  at  $\sqrt{s} = 10$  TeV. By contrast the PWM has nearly 2 TeV squarks and gluinos and requires over a 100 fold increase in luminosity to reach a comparable event rate in this channel. Thus after  $100 \text{ fb}^{-1}$  of integrated luminosity the PWM results in only 440 multijet events with  $\cancel{E}_T \geq 250$  GeV. This is illustrated in Figure (5) where the effective mass, defined as the scalar sum of the transverse momenta of the four hardest jets in the event plus the missing transverse energy, is plotted for events satisfying the cuts described above for the multijet channel. The signal for the HWM is clearly discernible above the Standard Model background after  $5 \text{ fb}^{-1}$ . For comparison we plot the same distribution for the PWM after  $100 \text{ fb}^{-1}$ .

*Experimental Challenges of the PWM Model:* The suppression of leptonic final states for both models, especially the trilepton channel, is the result of the small mass difference between the low-lying electroweak gaugino states which causes leptonic decay products to be generally quite soft. This is particularly severe for the wino-like scenario (the PWM). We note that the total (leading order) supersymmetric cross section for the PWM is still

Object Cuts (GeV)	HWM		PWM	
	Events	$S/\sqrt{B}$	Events	$S/\sqrt{B}$
$p_T^{\text{jet}} \geq 150, \cancel{E}_T \geq 150$	1994	2.13	3442	3.68
$p_T^{\text{jet}} \geq 200, \cancel{E}_T \geq 150$	1302	2.52	1983	3.84
$p_T^{\text{jet}} \geq 150, \cancel{E}_T \geq 200$	1334	2.53	2147	4.08
$p_T^{\text{jet}} \geq 200, \cancel{E}_T \geq 200$	1241	2.58	1904	3.95
$p_T^{\text{jet}} \geq 150, \cancel{E}_T \geq 300$	659	3.57	771	4.17

TABLE VI: Monojet signature for the HWM and the PWM: Event counts are after  $100 \text{ fb}^{-1}$  of integrated luminosity for various choices of cuts on total  $\cancel{E}_T$  and jet  $p_T$ . All signatures involve a lepton veto and require no other jets in the event with  $p_T^{\text{jet}} \geq 20$  GeV. No transverse sphericity cut was applied in any of these signatures.

a healthy 2.3 pb (to be compared with 7.4 pb for the HWM). The lack of a signal here is largely the result of an inability to trigger on events in which light electroweak gauginos are produced (99% of the total SUSY production cross-section) and the absence of hard leptons in the decay products of these states. These difficulties are common to phenomenological studies of models where the mass gaps between sparticles are small [20, 59, 60, 61] such as in models with anomaly-mediated supersymmetry breaking (AMSB) [62] which share many of the same features in the gaugino sector [63, 64] as the PWM.

Nevertheless, some signatures unique to this scenario can be explored with sufficient integrated luminosity. For example, one can look for events which pass the initial  $\cancel{E}_T$  trigger, but which have no leptons or energetic jets. Such events predominantly arise from direct production of  $\tilde{\chi}_1^\pm$  and/or  $\tilde{\chi}_{1,2}^0$  states whose decay products produce only very soft objects. If the mass difference  $\Delta m = m_{\tilde{\chi}_1^\pm} - m_{\tilde{\chi}^0}$  is sufficiently small the chargino will travel a macroscopic distance before decaying. An offline analysis may then reveal events with tracks in the inner layers of the detector which abruptly end, leaving no further leptonic tracks or calorimeter activity [65, 66, 67]. In the extreme limit of a pure-wino LSP, as in the AMSB models, this mass difference is typically the size of the pion mass, *i.e.*  $\mathcal{O}(m_\pi)$  and the distance traveled can be several centimeters. In the case of the PWM, however, the mass difference is roughly twice the pion mass and the typical decay length will be such that the decays will appear prompt and few events will reveal a displaced vertex. More promising is to consider events with a single high- $p_T$  jet and large missing transverse energy. Such events can arise from initial state radiation in electroweak gaugino production, or in cases where the lightest chargino or neutralino is produced in association with a gluino or squark. This particular ‘monojet’ channel has relatively large event rates for both the HWM and PWM, with the primary Standard Model background coming from  $W$ +jets production. Event rates and signal significance for various jet  $p_T$  and  $\cancel{E}_T$  cuts are given in Table (VI). More detailed analyses of similar models show that such events can be

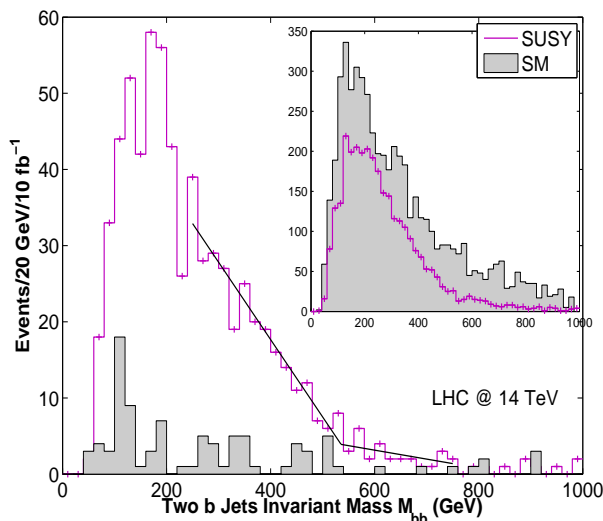


FIG. 6: The invariant mass distribution of 2 b-jets events for HWM where the LSP contains substantial Higgsino and wino components. Shaded histograms represents the Standard Model backgrounds. The solid lines are the best fit functions for the SUSY signal near the endpoint. The endpoint is estimated to be  $\sim 530$  GeV based on the linear fitting functions. The embedded window shows the mass distributions for both SUSY and SM, when one requires a 200 GeV missing energy cut. In order to suppress the Standard Model background, we increase the missing energy cut to 400 GeV and add two additional conditions: (1) lepton veto; (2) at least 2 more jets besides the 2 b-tagged jets.

bona-fide discovery modes in scenarios of this type [68].

*Measuring Sparticle Masses in the HWM Model:* For the mixed Higgsino-wino model (HWM) a sufficient number of events can be obtained even with a low integrated luminosity which will allow one to determine the properties of the superpartner spectrum and can confirm the features of Table (IV) – particularly those with direct relevance to the calculation of the thermal relic abundance and positron yield in cosmic rays. Thus even with  $10 \text{ fb}^{-1}$  it should be possible to get a reasonable estimate of the gluino mass by considering events with precisely two b-tagged jets. As the gluino is relatively light it would be produced in significant amounts and the invariant mass distribution of b-jets produced in its three-body decays will reveal a kink which allows one to determine the lower limit on the gluino mass knowing the LSP mass [69], *i.e.*  $m_{\tilde{g}} \geq (M_{\text{inv}}^{bb})^{\text{kink}} + m_{\tilde{\chi}^0}$ . Over 3000 events with two b-jets satisfying  $p_T^{\text{jet}} \geq 60$  GeV and  $\cancel{E}_T \geq 200$  GeV were produced in our  $10 \text{ fb}^{-1}$  sample for the HWM. With these cuts, the Standard Model background, arising mostly from  $t\bar{t}$  events, is comparable to the signal as is clear from the inset of Figure (6). To reduce this background we veto events with isolated leptons, require two additional jets without b-tags, each satisfying  $p_T^{\text{jet}} \geq 60$ , and increase the missing transverse energy cut from 200 GeV to 400 GeV. This

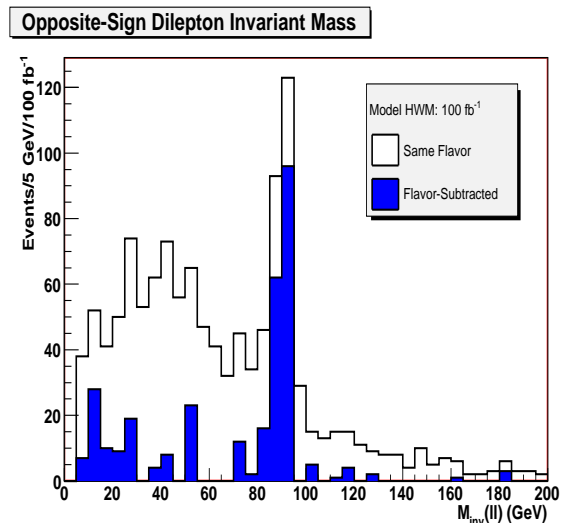


FIG. 7: Dilepton invariant mass distributions for the HWM after  $100 \text{ fb}^{-1}$ . The unshaded histogram gives the invariant mass distribution for events with precisely two opposite-sign leptons of the same flavor (electron or muon). The shaded histogram gives the flavor-subtracted distribution which results when the opposite-sign, opposite-flavor distribution is subtracted from the same-flavor distribution.

reduces the signal sample by approximately a factor of four, but the Standard Model background is now reduced to manageable levels. This is displayed in the main panel of Figure (6) where  $(M_{\text{inv}}^{bb})^{\text{kink}} \sim 500$  GeV, which gives  $m_{\tilde{g}} \gtrsim 700$  GeV, which is consistent with the true gluino mass of 707 GeV in this model.

Of even more relevance is the relatively small mass gap between the two lightest neutralinos  $\tilde{\chi}_2^0$  and  $\tilde{\chi}^0$ . While not as severe as in the wino-like case of the PWM, the mass difference is still small enough that the number of energetic leptons coming from the final stages of sparticle cascade decays will be suppressed relative to the number expected from more universal models. The reduction in events with two or more energetic, isolated leptons will significantly degrade the ability to make measurements of mass differences using the edges of various kinematic distributions. For example, a typical strategy for accessing the mass difference between light neutralinos is to form the flavor-subtracted dilepton invariant mass for events with at least two jets satisfying  $p_T^{\text{jet}} \geq 60$  GeV, at least 200 GeV of  $\cancel{E}_T$  and two opposite-sign leptons [70]. The invariant mass distribution formed from the subset involving two leptons of opposite flavor is subtracted from that involving two of the same flavor, *i.e.*, the combination  $(e^+e^- + \mu^+\mu^- - e^+\mu^- - e^-\mu^+)$ , to reduce background. In Fig.(7) we plot the invariant mass of same-flavor, opposite-sign leptons in two-lepton events for HWM after  $100 \text{ fb}^{-1}$  as well as the flavor-subtracted distribution. Note the small number of events which remain after the subtraction procedure has been

performed. Nevertheless, the beginnings of a feature in the low-energy bins can be discerned which is consistent with the mass differences between the low-lying gauginos in this model. Additional statistics and more careful analysis techniques will be needed to make strong statements about the neutralino masses in this model.

*ILC Implications:* The ideal machine to study the spectroscopy of the light gauginos and to confirm the model as a potential explanation for the PAMELA positron excess would be at a potential International Linear Collider (ILC). We emphasize that a linear collider operating at a center-of-mass energy of 500 GeV would be sufficient to study the closely-spaced lightest neutralinos and lightest charginos of either model. For the case of the pure wino model (PWM) a future linear collider will be essential for resolving the presence of two nearly-degenerate states near 200 GeV and for studying their couplings. The prospects for both models at the ILC are quite good with  $\sigma(e^+e^- \rightarrow \text{SUSY}) = O(0.1)$  pb for both models. Finally, it is worth pointing out that for both models there is the distinct possibility of observing a degenerate cluster of  $Z'$  bosons with masses of the order of the lightest chargino mass. This will only be possible if the decays of such additional  $Z'$  bosons into hidden sector matter states are forbidden or largely suppressed. In such cases they would appear as sharp resonances in Drell-Yan processes and should be discernible at the LHC with sufficient luminosity. Observation of such states would be a spectacular confirmation of the  $B_{C_0}$  mechanism of generating the correct neutralino relic density by thermal means for the HWM model.

## IX. CONCLUSIONS

The positron excess observed in the PAMELA satellite experiment has spawned various mechanisms to explain this effect. An interesting possibility relates to the positron excess arising from the annihilation of dark matter in the galaxy. An adequate explanation of this phenomenon within a particle physics model then would require a simultaneous fit both to the WMAP data regarding the density of cold dark matter as well as to the PAMELA data. Often it turns out that models that give the desired relic density give too small a  $\langle\sigma v\rangle$  in the galaxy to explain the PAMELA excess. Alternately, models which produce an adequate  $\langle\sigma v\rangle$  and explain the

PAMELA excess fail to produce the proper relic density. To reconcile the two phenomena typically the following mechanisms have been proposed: (i) For models that generate the right relic density but give too small a  $\langle\sigma v\rangle$  the Sommerfeld enhancement or the Breit-Wigner pole enhancement of  $\langle\sigma v\rangle$  can explain both sets of data; (ii) For models which give an adequate  $\langle\sigma v\rangle$  to explain the PAMELA excess but give too small a relic density, a non-thermal mechanism is taken to produce the proper relic abundance.

In this paper we have carried out an analysis of a distinctly different mechanism which can generate the proper relic density for the second type of models, *i.e.*, models where  $\langle\sigma v\rangle$  is large enough to explain the PAMELA excess but the relic density needs an enhancement. We illustrate this mechanism within the framework of nonuniversal SUGRA models with an extended hidden  $U(1)_X^n$  gauge symmetry. The extension along with conditions of mass degeneracy in the hidden sector gives rise to predictions which match the PAMELA data and the predicted relic density is consistent with the WMAP data with a mixed Higgsino-wino LSP. The anti-proton and the gamma ray fluxes emanating from the annihilation of dark matter in the galaxy are found to be compatible with data. Implications of the model for the direct detection of dark matter and some of its collider signatures were also discussed. The model is testable on both fronts. Specifically the mixed Higgsino-wino LSP model is testable at the LHC with just  $1 \text{ fb}^{-1}$  of data. While the analysis was done in the framework of nonuniversal SUGRA models, the results of the analysis are valid in a broad class of models including string and D-brane models as long there is an LSP with mass in the proper range and a suitable admixture of Higgsino-wino components with an appropriate degeneracy in the hidden sector. Finally, we note that we have not made an attempt here to fit the FERMI-LAT  $e^+ + e^-$  result [2]. Such a fit can be accommodated by assuming that the high energy flux is a consequence of pulsars or mixed dark matter and pulsar contributions [13, 71].

*Acknowledgments:* This research is supported in part by NSF Grants No. PHY-0757959 and No. PHY-0653587 (Northeastern) and No. PHY-0653342 (Stony Brook), and by the US Department of Energy (DOE) under grant DE-FG02-95ER40899 (Michigan).

- 
- [1] O. Adriani *et al.* [PAMELA Collaboration], *Nature* **458**, 607 (2009); *Phys. Rev. Lett.* **102**, 051101 (2009).  
 [2] A. A. Abdo *et al.* [The Fermi LAT Collaboration], *Phys. Rev. Lett.* **102**, 181101 (2009); See also, J. Chang *et al.*, *Nature* **456**, 362 (2008).  
 [3] M. Cirelli, R. Franceschini and A. Strumia, *Nucl. Phys. B* **800**, 204 (2008); M. Cirelli, M. Kadastik, M. Raidal, A. Strumia, *Nucl. Phys. B* **813**, 1 (2009).  
 [4] P. Grajek, G. Kane, D. J. Phalen, A. Pierce and S. Watson, arXiv:0807.1508 [hep-ph]; *Phys. Rev. D* **79**, 043506 (2009); G. Kane, R. Lu and S. Watson, arXiv:0906.4765 [astro-ph.HE].  
 [5] J. Hisano, M. Kawasaki, K. Kohri and K. Nakayama, *Phys. Rev. D* **79**, 063514 (2009).  
 [6] D. Feldman, Z. Liu and P. Nath, *Phys. Rev. D* **79**, 063509 (2009); M. Ibe, H. Murayama and T. T. Yanagida, *Phys. Rev. D* **79**, 095009 (2009); W. L. Guo and Y. L. Wu, *Phys. Rev. D* **79**, 055012 (2009); W. L. Guo and X. Zhang, arXiv:0904.2451 [hep-ph]. M. Ibe, Y. Nakayama, H. Murayama and T. T. Yanagida,

- arXiv:0902.2914 [hep-ph]; X. J. Bi, X. G. He and Q. Yuan, arXiv:0903.0122 [hep-ph]; F. Y. Cyr-Racine, S. Profumo and K. Sigurdson, arXiv:0904.3933 [astro-ph.CO]; For related work see: D. Feldman, Z. Liu and P. Nath, Phys. Rev. D **75**, 115001 (2007); M. Pospelov and A. Ritz, Phys. Lett. B **671**, 391 (2009); W. Shepherd, T. M. P. Tait and G. Zaharijas, Phys. Rev. D **79**, 055022 (2009).
- [7] V. Barger, W. Y. Keung, D. Marfatia and G. Shaughnessy, Phys. Lett. B **672**, 141 (2009); Y. Nomura and J. Thaler, arXiv:0810.5397 [hep-ph]; J. Zhang, X. J. Bi, J. Liu, S. M. Liu, P. f. Yin, Q. Yuan and S. H. Zhu, arXiv:0812.0522 [astro-ph]; P. H. Frampton and P. Q. Hung, Phys. Lett. B **675**, 411 (2009); S. L. Chen, R. N. Mohapatra, S. Nussinov and Y. Zhang, Phys. Lett. B **677**, 311 (2009); K. Cheung, P. Y. Tseng and T. C. Yuan, arXiv:0902.4035 [hep-ph]; I. Gogoladze, N. Okada and Q. Shafi, arXiv:0904.2201 [hep-ph]; J. Hisano, M. Kawasaki, K. Kohri, T. Moroi and K. Nakayama, Phys. Rev. D **79**, 083522 (2009); F. Chen, J. M. Cline and A. R. Frey, arXiv:0907.4746 [hep-ph].
- [8] H. Davoudiasl, arXiv:0904.3103 [hep-ph]; R. Brandenberger, Y. F. Cai, W. Xue and X. m. Zhang, arXiv:0901.3474 [hep-ph]; Q. H. Cao, E. Ma and G. Shaughnessy, Phys. Lett. B **673**, 152 (2009); C. R. Chen, M. M. Nojiri, S. C. Park, J. Shu and M. Takeuchi, arXiv:0903.1971 [hep-ph]; S. C. Park and J. Shu, Phys. Rev. D **79**, 091702 (2009); L. Bergstrom, arXiv:0903.4849 [hep-ph]; C. B. Braeuninger and M. Cirelli, Phys. Lett. B **678**, 20 (2009); Q. Yuan, X. J. Bi, J. Liu, P. F. Yin, J. Zhang and S. H. Zhu, arXiv:0905.2736 [astro-ph.HE]; N. Okada and T. Yamada, arXiv:0905.2801 [hep-ph]; C. H. Chen, arXiv:0905.3425 [hep-ph]; P. H. Gu, H. J. He, U. Sarkar and X. m. Zhang, arXiv:0906.0442 [hep-ph]; K. Kohri, J. McDonald and N. Sahu, arXiv:0905.1312 [hep-ph]; C. Balazs, N. Sahu and A. Mazumdar, arXiv:0905.4302 [hep-ph].
- [9] A. Ibarra, A. Ringwald, D. Tran and C. Weniger, arXiv:0903.3625 [hep-ph]; C. R. Chen, M. M. Nojiri, F. Takahashi and T. T. Yanagida, arXiv:0811.3357 [astro-ph]; E. Nardi, F. Sannino and A. Strumia, JCAP **0901**, 043 (2009); J. Liu, P. f. Yin and S. h. Zhu, arXiv:0812.0964 [astro-ph]; C. R. Chen, K. Hamaguchi, M. M. Nojiri, F. Takahashi and S. Torii, JCAP **0905**, 015 (2009); K. Ishiwata, S. Matsumoto and T. Moroi, Phys. Rev. D **79**, 043527 (2009); JHEP **0905**, 110 (2009); X. Chen, arXiv:0902.0008 [hep-ph]; H. Fukuoka, J. Kubo and D. Suematsu, Phys. Lett. B **678**, 401 (2009).
- [10] L. Bergstrom, T. Bringmann and J. Edsjo, Phys. Rev. D **78**, 103520 (2008); R. Harnik and G. D. Kribs, arXiv:0810.5557 [hep-ph]; R. Allahverdi, B. Dutta, K. Richardson-McDaniel and Y. Santoso, Phys. Rev. D **79**, 075005 (2009); Phys. Lett. B **677**, 172 (2009); H. S. Goh, L. J. Hall and P. Kumar, JHEP **0905**, 097 (2009); C. H. Chen, C. Q. Geng and D. V. Zhuridov, arXiv:0905.0652 [hep-ph]; Y. Bai, M. Carena and J. Lykken, arXiv:0905.2964 [hep-ph]; D. A. Demir, L. L. Everett, M. Frank, L. Selbuz and I. Turan, arXiv:0906.3540 [hep-ph].
- [11] G. Bertone, M. Cirelli, A. Strumia and M. Taoso, JCAP **0903**, 009 (2009); L. Bergstrom, G. Bertone, T. Bringmann, J. Edsjo and M. Taoso, Phys. Rev. D **79**, 081303 (2009); W. de Boer, arXiv:0901.2941 [hep-ph]; M. Kawasaki, K. Kohri and K. Nakayama, arXiv:0904.3626 [astro-ph.CO]; X. J. Bi, R. Brandenberger, P. Gondolo, T. Li, Q. Yuan and X. Zhang, arXiv:0905.1253 [hep-ph]; R. Essig, N. Sehgal and L. E. Strigari, Phys. Rev. D **80**, 023506 (2009).
- [12] C. Delaunay, P. J. Fox and G. Perez, JHEP **0905**, 099 (2009); J. Hisano, K. Nakayama and M. J. S. Yang, Phys. Lett. B **678**, 101 (2009); M. R. Buckley, K. Freese, D. Hooper, D. Spolyar and H. Murayama, arXiv:0907.2385 [astro-ph.HE].
- [13] H. Yuksel, M. D. Kistler and T. Stanev, Phys. Rev. Lett. **103** 051101 (2009); D. Hooper, P. Blasi and P. D. Serpico, JCAP **0901**, 025 (2009); S. Profumo, arXiv:0812.4457 [astro-ph]; D. Hooper, A. Stebbins and K. M. Zurek, arXiv:0812.3202 [hep-ph]; E. Borriello, A. Cuoco and G. Miele, Astrophys. J. **699**, L59 (2009). V. Barger, Y. Gao, W. Y. Keung, D. Marfatia and G. Shaughnessy, arXiv:0904.2001 [hep-ph]; See also the last Ref. of [4].
- [14] A. H. Chamseddine, R. Arnowitt and P. Nath, Phys. Rev. Lett. **49** (1982) 970; P. Nath, R. L. Arnowitt and A. H. Chamseddine, Nucl. Phys. B **227**, 121 (1983); L. Hall, J. Lykken and S. Weinberg, Phys. Rev. **D27**, 2359 (1983); For reviews see: P. Nath, R. L. Arnowitt and A. H. Chamseddine, "Applied N=1 Supergravity," Trieste Particle Phys.1983:1 (QCD161:W626:1983), World Scientific (July 1984); H. P. Nilles, Phys. Rept. **110**, 1 (1984); P. Nath, arXiv:hep-ph/0307123.
- [15] M. S. Turner and F. Wilczek, Phys. Rev. D **42**, 1001 (1990).
- [16] D. N. Spergel *et al.* [WMAP Collaboration], Astrophys. J. Suppl. **170**, 377 (2007); E. Komatsu *et al.* [WMAP Collaboration], Astrophys. J. Suppl. **180**, 330 (2009).
- [17] T. Moroi and L. Randall, Nucl. Phys. B **570**, 455 (2000); G. L. Kane, L. T. Wang and J. D. Wells, Phys. Rev. D **65**, 057701 (2002); B. S. Acharya, P. Kumar, K. Bobkov, G. Kane, J. Shao and S. Watson, JHEP **0806**, 064 (2008).
- [18] J.R. Ellis, K. Enqvist, D.V. Nanopoulos and K. Tamvakis, Phys. Lett. B **155**, 381 (1985); M. Drees, Phys. Lett. B **158**, 409 (1985).
- [19] A. Corsetti and P. Nath, Phys. Rev. D **64**, 125010 (2001); U. Chattopadhyay and P. Nath, Phys. Rev. D **65**, 075009 (2002); G. L. Kane, J. D. Lykken, S. Mrenna, B. D. Nelson, L. T. Wang and T. T. Wang, Phys. Rev. D **67**, 045008 (2003); A. Birkedal-Hansen and B. D. Nelson, Phys. Rev. D **67**, 095006 (2003); D. G. Cerdeno and C. Munoz, JHEP **0410**, 015 (2004); H. Baer, A. Mustafayev, S. Profumo, A. Belyaev and X. Tata, JHEP **0507**, 065 (2005); S. F. King, J. P. Roberts and D. P. Roy, JHEP **0710**, 106 (2007).
- [20] A. Birkedal-Hansen and B. D. Nelson, Phys. Rev. D **64**, 015008 (2001).
- [21] D. Feldman, Z. Liu and P. Nath, Phys. Lett. B **662**, 190 (2008); H. Baer, A. Mustafayev, E. K. Park and X. Tata, JHEP **0805**, 058 (2008); D. Feldman, Z. Liu and P. Nath, JHEP **0804**, 054 (2008); B. Altunkaynak, M. Holmes and B. D. Nelson, JHEP **0810**, 013 (2008); S. P. Martin, Phys. Rev. D **78** (2008) 055019; S. Bhattacharya, A. Datta and B. Mukhopadhyaya, Phys. Rev. D **78**, 115018 (2008); U. Chattopadhyay and D. Das, Phys. Rev. D **79**, 035007 (2009); B. Altunkaynak, P. Grajek, M. Holmes, G. Kane and B. D. Nelson, JHEP **0904**, 114 (2009); S. P. Martin, arXiv:0903.3568 [hep-ph]; D. Feldman, Z. Liu and P. Nath, arXiv:0905.1148 [hep-ph]; M. Holmes and B. D. Nelson, JCAP **0907**, 019



- (2009); S. Bhattacharya, U. Chattopadhyay, D. Choudhury, D. Das and B. Mukhopadhyaya, arXiv:0907.3428 [hep-ph].
- [22] J. Hisano, S. Matsumoto and M. M. Nojiri, Phys. Rev. Lett. **92**, 031303 (2004).
- [23] S. Cassel, D. M. Ghilencea and G. G. Ross, arXiv:0903.1118 [hep-ph].
- [24] D. Feldman, B. Kors and P. Nath, Phys. Rev. D **75**, 023503 (2007) [arXiv:hep-ph/0610133]; P. Anastasopoulos, F. Fucito, A. Lionetto, G. Pradisi, A. Racioppi and Y. S. Stanev, Phys. Rev. D **78**, 085014 (2008) F. Fucito, A. Lionetto, A. Mammarella and A. Racioppi, arXiv:0811.1953 [hep-ph]; C. Coriano, M. Guzzi, N. Irges and A. Mariano, Phys. Lett. B **671** (2009) 87.
- [25] S. Profumo and A. Provenza, JCAP **0612**, 019 (2006); [arXiv:hep-ph/0609290].
- [26] K. Griest and D. Seckel, Phys. Rev. D **43**, 3191 (1991).
- [27] P. Gondolo, J. Edsjo, P. Ullio, L. Bergstrom, M. Schelke and E. A. Baltz, JCAP **0407**, 008 (2004); G. Belanger, F. Boudjema, A. Pukhov and A. Semenov, Comput. Phys. Commun. **180**, 747 (2009).
- [28] B. Kors and P. Nath, Phys. Lett. B **586**, 366 (2004); JHEP **0412**, 005 (2004); JHEP **0507**, 069 (2005); D. Feldman, Z. Liu and P. Nath, JHEP **0611**, 007 (2006); K. Cheung and T. C. Yuan, JHEP **0703**, 120 (2007); arXiv:0710.2005 [hep-ph]; D. Feldman, Z. Liu and P. Nath, AIP Conf. Proc. **939**, 50 (2007).
- [29] D. Feldman, Z. Liu and P. Nath, Phys. Rev. Lett. **97** (2006) 021801; See also J. Kumar and J. D. Wells, Phys. Rev. D **74**, 115017 (2006) W. F. Chang, J. N. Ng and J. M. S. Wu, Phys. Rev. D **74**, 095005 (2006); S. Gopalakrishna, S. J. Lee and J. D. Wells, arXiv:0904.2007 [hep-ph].
- [30] J. Hisano, S. Matsumoto, O. Saito and M. Senami, Phys. Rev. D **73** (2006) 055004.
- [31] T. Delahaye, R. Lineros, F. Donato, N. Fornengo and P. Salati, Phys. Rev. D **77**, 063527 (2008); P. Brun, G. Bertone, J. Lavalle, P. Salati, R. Taillet, Phys. Rev. D **76**, 083506 (2007).
- [32] M. Kamionkowski and S. M. Koushiappas, Phys. Rev. D **77**, 103509 (2008).
- [33] M. S. Longair, *Cambridge, UK: Univ. Pr. (1994)*.
- [34] J. F. Navarro, C. S. Frenk and S. D. M. White, Astrophys. J. **490**, 493 (1997); B. Moore et.al, Mon. Not. Roy. Astron. Soc. **310**, 1147 (1999).
- [35] G. Corcella *et al.*, JHEP **0101**, 010 (2001).
- [36] I. V. Moskalenko and A. W. Strong, Astrophys. J. **493**, 694 (1998); E. A. Baltz and J. Edsjo, Phys. Rev. D **59**, 023511 (1998).
- [37] A. Bottino, C. Favero, N. Fornengo and G. Mignola, Astropart. Phys. **3**, 77 (1995).
- [38] D. Maurin, F. Donato, R. Taillet and P. Salati, Astrophys. J. **555**, 585 (2001).
- [39] L. Bergstrom, J. Edsjo and P. Ullio, Astrophys. J. **526**, 215 (1999).
- [40] T. Bringmann and P. Salati, Phys. Rev. D **75**, 083006 (2007).
- [41] A. Bruno, PhD Thesis, Universita Degli Studi Di Bari.
- [42] M. Ricci, Invited Talk at SUSY 09, Northeastern University, Boston.
- [43] S. Orito *et al.* [BESS Collaboration], Phys. Rev. Lett. **84**, 1078 (2000); See also: T. Maeno *et al.* [BESS Collaboration], Astropart. Phys. **16**, 121 (2001); M. Boezio *et al.* [WiZard/CAPRICE Collaboration], Astrophys. J. **561**, 787 (2001).
- [44] L. Bergstrom, P. Ullio and J. H. Buckley, Astropart. Phys. **9**, 137 (1998).
- [45] P. Meade, M. Papucci, A. Strumia and T. Volansky, arXiv:0905.0480 [hep-ph]; M. Cirelli and P. Panci, arXiv:0904.3830 [astro-ph.CO].
- [46] V. Berezhinsky, A. Bottino and G. Mignola, Phys. Lett. B **325**, 136 (1994).
- [47] N. Fornengo, L. Pieri and S. Scopel, Phys. Rev. D **70**, 103529 (2004).
- [48] A. W. Strong, I. V. Moskalenko and O. Reimer, Astrophys. J. **613**, 962 (2004).
- [49] L. Bergstrom, T. Bringmann, M. Eriksson and M. Gustafsson, Phys. Rev. Lett. **95**, 241301 (2005).
- [50] S. D. Hunter *et al.*, Astrophys. J. **481**, 205 (1997).
- [51] N. Giglietto, Les Rencontres de Physique, de la Vallée D'Aoste; La Thuile 2009.
- [52] B. Winer, Plenary Talk at SUSY 09, Northeastern University, Boston; T. A. Porter and f. t. F. Collaboration, arXiv:0907.0294 [astro-ph.HE].
- [53] L. Bergstrom and P. Ullio, Nucl. Phys. B **504**, 27 (1997); Z. Bern, P. Gondolo and M. Perelstein, Phys. Lett. B **411**, 86 (1997).
- [54] B. C. Allanach, Comput. Phys. Commun. **143**, 305 (2002) Present version 3.02 (2009).
- [55] J. Hisano, S. Matsumoto, M. M. Nojiri and O. Saito, Phys. Rev. D **71**, 015007 (2005).
- [56] P. Skands *et al.*, JHEP **0407**, 036 (2004); PGS-4, J. Conway *et al.*
- [57] G. L. Bayatian *et al.* [CMS Collaboration], J. Phys. G **34**, 995 (2007).
- [58] H. Baer, C. h. Chen, F. Paige and X. Tata, Phys. Rev. D **52**, 2746 (1995); H. Baer, C. h. Chen, F. Paige and X. Tata, Phys. Rev. D **53**, 6241 (1996) [arXiv:hep-ph/9512383].
- [59] U. Chattopadhyay, D. Das, P. Konar and D. P. Roy, Phys. Rev. D **75**, 073014 (2007).
- [60] F. E. Paige and J. D. Wells, arXiv:hep-ph/0001249.
- [61] H. Baer, J. K. Mizukoshi and X. Tata, Phys. Lett. B **488**, 367 (2000).
- [62] L. Randall and R. Sundrum, Nucl. Phys. B **557**, 79 (1999); [arXiv:hep-th/9810155]. G. F. Giudice, M. A. Luty, H. Murayama and R. Rattazzi, JHEP **9812**, 027 (1998); [arXiv:hep-ph/9810442].
- [63] M. K. Gaillard, B. D. Nelson and Y. Y. Wu, Phys. Lett. B **459** (1999) 549 [arXiv:hep-th/9905122].
- [64] J. A. Bagger, T. Moroi and E. Poppitz, JHEP **0004**, 009 (2000) [arXiv:hep-th/9911029].
- [65] C. H. Chen, M. Drees and J. F. Gunion, Phys. Rev. Lett. **76**, 2002 (1996).
- [66] J. L. Feng, T. Moroi, L. Randall, M. Strassler and S. f. Su, Phys. Rev. Lett. **83**, 1731 (1999).
- [67] T. Gherghetta, G. F. Giudice and J. D. Wells, Nucl. Phys. B **559**, 27 (1999).
- [68] A. J. Barr, C. G. Lester, M. A. Parker, B. C. Allanach and P. Richardson, JHEP **0303**, 045 (2003).
- [69] R. Kitano and Y. Nomura, Phys. Rev. D **73**, 095004 (2006).
- [70] I. Hinchliffe, F. E. Paige, M. D. Shapiro, J. Soderqvist and W. Yao, Phys. Rev. D **55**, 5520 (1997).
- [71] D. Grasso *et al.* [FERMI-LAT Collaboration], arXiv:0905.0636 [astro-ph.HE]; L. Bergstrom, J. Edsjo and G. Zaharijas, arXiv:0905.0333 [astro-ph.HE].